Organic & Biomolecular Chemistry

ROYAL SOCIETY OF CHEMISTRY

PAPER

View Article Online
View Journal | View Issue

Cite this: *Org. Biomol. Chem.*, 2025, **23**, 5826

Triplet-sensitized cyclobutane pyrimidine dimer damage and crosslinks in DNA: filling the triplet energy gap between xanthone and thioxanthone†

Sebastian Häcker, [a] Julian Amir Moghtader, [b] Christoph Kerzig [b] and Hans-Achim Wagenknecht *[a]

Thioxanthones are tunable photosensitizers used for studying the formation of triplet-induced cyclobutane pyrimidine dimer (CPD) damage in DNA. To probe the gap between the triplet energy of xanthone (310 kJ mol^{-1}) and of thioxanthone (265 kJ mol^{-1}), we synthesized two new C-nucleosides with two differently modified thioxanthones. Ternary and photoactive DNA architectures were prepared with these C-nucleosides to analyze the CPD formation quantitatively. The dimethoxy-substituted thioxanthone as a photosensitizer has a high triplet energy (288 kJ mol^{-1}). We observed the CPD formation over up to 6 A–T pairs in DNA, and the distance dependence is characterized by a low β-value of 0.02 Å^{-1}, indicating energy hopping over the A–T pairs. The triplet energy of the chloro-and methoxy-modified photosensitizer is low (273 kJ mol^{-1}) and only slightly above the threshold for DNA photosensitization set by the triplet energy of T in DNA (267 kJ mol^{-1}). Here, only low amounts of CPDs were obtained because the energy difference compared to T is very small. These results show clearly that the triplet energy of the photosensitizer incorporated into the DNA is decisive for not only whether CPDs can be induced at all but also how much CPDs are formed; the higher the triplet energy of the photosensitizer, the more CPDs are formed.

Received 10th April 2025,
Accepted 19th May 2025

DOI: 10.1039/d5ob00599j

rsc.li/obc

Introduction

Sunlight absorption leads to genomic DNA damage that may cause skin cancer.[1–3] To get the best possible insights for understanding the excited state dynamics in DNA, it is crucial to elucidate all pathways to DNA photodamage, from both singlet and triplet states.[4–6] The direct excitation of DNA by UV-B light induces singlet excitons. These charge-separated states delocalize over several base pairs[7–11] and recombine in a few hundred ps. This protects DNA from UV photodamage by direct excitation.[12] Cyclobutane pyrimidine dimers (CPDs) are such primary forms of DNA photodamage,[4–6] formed from the single states of adjacent thymidines in a nearly barrier-free and extremely fast [2 + 2]-cycloaddition reaction,[13] and are considered to be some of the molecular origins of skin cancer, among others in photocarcinogenesis.[1,3,14] In contrast to these well-studied singlet photochemical processes leading to DNA damage, triplet photochemistry in DNA and the associated pathways causing DNA photodamage are less well explored. The reason for this is the difficulty of regiospecific excitation and population of triplet states in DNA. A decisive parameter is the triplet energy of the 2′-deoxynucleotides as DNA components. The triplet states of DNA are accessible through photosensitization using organic chromophores as energy donors.[15,16] Compared to the other 2′-deoxynucleotides, thymidine (T) is the primary target for triplet photochemistry in DNA as it has the lowest triplet energy in the range between E_T = 310 kJ mol^{-1} for thymidine monophosphate and E_T = 267 kJ mol^{-1} in double-stranded DNA.[17] This indicates that the environment can have a major influence on the triplet energy of the DNA components. Theoretical molecular dynamics simulations showed that polarization effects lower the triplet energy of T to only E_T = 300 kJ mol^{-1}, when the stacking with the four different DNA bases is regarded.[18] Photosensitizers with sufficient triplet energy are able to induce triplet states in DNA, which might lead to the formation of CPDs.[19] Xanthones and thioxanthones are well-established photosensitizers with a remarkable broad range of triplet energies.[20–23] Xanthone shows a triplet energy of E_T = 310 kJ mol^{-1}, identical to the triple energy of T monophosphate and therefore sufficiently high for DNA sensitization.[21] We showed that xanthone is able

[a]*Institute of Organic Chemistry, Karlsruhe Institute of Technology (KIT), Fritz-Haber-Weg 6, 76131 Karlsruhe, Germany. E-mail: Wagenknecht@kit.edu*
[b]*Department of Chemistry, Johannes Gutenberg University Mainz, Duesbergweg 10-14, 55128 Mainz, Germany*

†Electronic supplementary information (ESI) available: Materials and methods, synthesis of C-nucleosides **1** and **2**, DNA synthesis and purification, irradiation experiments, NMR and MS data, and spectroscopic results. See DOI: https://doi.org/10.1039/d5ob00599j

to not only sensitize triplet states in double-stranded DNA but also promote triplet energy transport to form CPDs at sites up to seven base pairs away. On the other hand, thioxanthone does not induce any triplet-sensitized CPDs in DNA due to its low triplet energy of E_T = 265 kJ mol^{-1}.[24] To fill the gap and obtain photosensitizers with triplet energies between these two critical values, E_T = 267 kJ mol^{-1} and 310 kJ mol^{-1}, we fine-tuned the photophysical properties of thioxanthones using chloro and methoxy substituents. Herein, we show the synthesis of two photosensitizers as C-nucleosides **1** and **2** with modified thioxanthones and their synthetic incorporation into DNA (Fig. 1). Using automated DNA synthesis based on phosphoramidite chemistry, both photosensitizers were incorporated at defined positions inside double-stranded DNA. The DNA triplet photochemistry can be probed selectively by excitation in the UV-A range where the DNA shows only a little extinction. The photosensitizers **1** and **2** were placed into ternary DNA architectures at different, precisely defined distances from two adjacent Ts that are not covalently linked *via* the phosphate backbone. The CPDs form an elongated DNA strand, which could be detected by HPLC on a quantitative level.

Results

Thionated chromophores are strong photosensitizers,[25] for instance thionated BODIPYs,[26] phenothiazines[27] and naphthalene diimides.[28] Thioxanthones have the potential to be optimal photosensitizers for studying the formation of CPD damage by energy transfer. In the literature, thioxanthone has already shown its efficacy as a photosensitizer in other [2 + 2] cycloadditions,[29–32] suggesting that thioxanthone should also be able to sensitize the [2 + 2] cycloaddition between two Ts in DNA, leading to the CPD damage. Triplet energies of unmodified thioxanthone, ranging from E_T = 263 kJ mol^{-1} to 274 kJ mol^{-1}, have been determined in the literature.[20–23] These values are very close to the triplet energy of T in DNA (E_T = 267 kJ mol^{-1}),[17] as determined by Miranda *et al.*, but may not be sufficient for the sensitization of CPD formation.[33] In fact, we recently evidenced that the C-nucleoside of thioxanthone cannot sensitize CPD formation in double-stranded DNA.[34] Hence, the triplet energy of thioxanthone in DNA must be lower than E_T = 267 kJ mol^{-1}. On the other hand, xanthone has a relatively high triplet energy of E_T = 310 kJ mol^{-1} and is able to sensitize CPD formation over a distance of up to seven base pairs.[24] In order to probe the triplet energy gap between xanthone and thioxanthone, we designed the C-nucleosides **1** and **2**. The difference in the positions of the glycosidic bond in the thioxanthones in **1** and **2** is the result of the synthetic access. Despite this structural difference, we assume that in both cases there is a coplanar orientation of the chromophore inside the DNA base stack. As a result, the A in the position of the "counterbase" might be pushed into an extrahelical position, which should not interfere with the photosensitization of the DNA along the double helix. Compared to thioxanthone, their triplet energy should be increased by functionalization with methoxy groups.[20] The C-nucleoside **1** was synthesized from the brominated precursor **6** of the chromophore (Scheme 1). It starts with thiosalicylic acid (**3**) prepared according to a literature procedure.[20] The acid **3** was activated *in situ* using thionyl chloride and sulfuryl chloride to the chlorosulfenyl benzoyl chloride **4**, which was not isolated. Upon adding $AlCl_3$, the intermediate **4** reacted with 3-bromobenzene to give the brominated thioxanthone **6** in a yield of 53%. Interestingly, the main product of this reaction was not thioxanthone **5**, which might be expected. Under the applied reaction conditions, sulfuryl chloride dissociates into SO_2 and Cl_2,

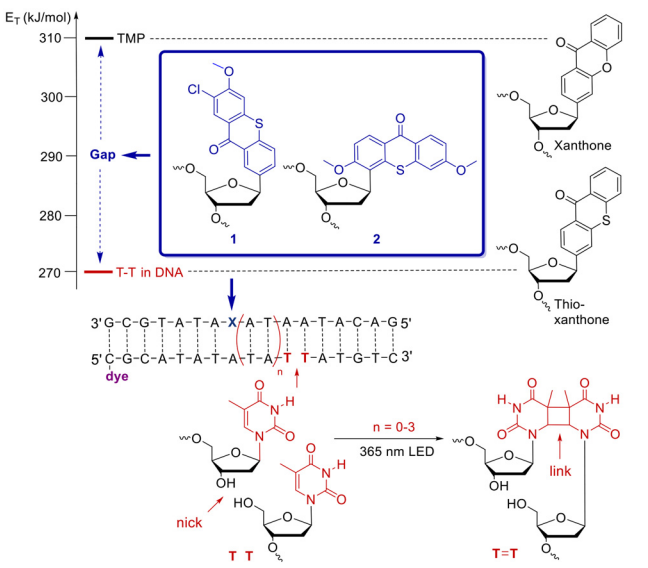

Fig. 1 Ternary DNA architectures with modified thioxanthones **1** and **2** as photosensitizers. The modified thioxanthones probe photochemically the gap of triplet energies E_T between xanthone (E_T = 310 kJ mol^{-1}) and thioxanthone (E_T < 270 kJ mol^{-1}), and thus between T monophosphate and T in DNA.

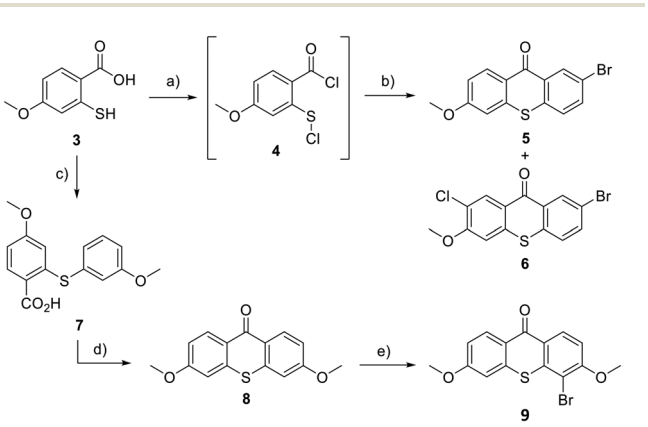

Scheme 1 Synthesis of the brominated precursors **6** and **9** for the synthesis of C-nucleosides **1** and **2**: (a) $SOCl_2$, SO_2Cl_2, bromobenzene, DMF, 110 °C → 10 °C, and 1.5 h. (b) $AlCl_3$, bromobenzene, 20 °C → 60 °C, and 1 h; (c) DMF, K_2CO_3, CuI, 145 °C, and 2.5 h. (d) $SOCl_2$, DCM, DMF, $AlCl_3$, rt, and 2 h. (d) $BTMABr_3$, $ZnCl_2$, AcOH, rt, and 12 h.

with the latter most likely acting as a chlorinating reagent in the presence of $AlCl_3$.[35,36] Due to the activating effect of the methoxy group, the aromatic ring is preferentially chlorinated at the *ortho*-position relative to the methoxy group, which is also favored by the *para*-located sulfur and the *meta*-located carbonyl group. For the synthesis of the brominated precursor **9** for C-nucleoside **2**, 3,6-dimethoxythioxanthone (**8**) was prepared from thiosalicylic acid (**3**) by an Ullmann coupling to thioether **7**, which was converted into **8** *via* an intramolecular Friedel–Crafts acylation reaction.[20] For selective bromination of **8**, the reaction was initially attempted using benzyltriethylammonium tribromide, but no conversion occurred. Therefore, the more reactive benzyltrimethylammonium tribromide ($BTMABr_3$) was used. Since $BTMABr_3$ is only slightly soluble in acetic acid, $ZnCl_2$ was added to improve solubility.[37] A complex between $BTMABr_3$ and $ZnCl_2$ is postulated to be the active species.[37] Bromination was observed at the 2- and 4-positions in a ratio of 1 : 4, although the 2-position would be preferred for steric reasons. It is conceivable that the active complex coordinates between the sulfur and the methoxy group, whereby bromination occurs preferentially at the 4-position. After recrystallization, product **9** was isolated in a yield of 43%.

The brominated thioxanthones **6** and **9** were converted into the C-nucleosides **1** and **2** and subsequently to the phosphoramidites **14** and **18** to synthetically incorporate them into oligonucleotides (Scheme 2). This approach enables precise distance determination of the CPD formation, as the photosensitizer replaces a natural 2′-deoxynucleotide and is thus specifically integrated into the DNA base stack by π–π stacking interactions. In comparison with conventional nucleosides, C-nucleosides are more stable against hydrolysis[38] which is good for the investigation of their photochemistry in DNA. For the C-nucleoside synthesis, the Heck coupling was applied.[24,39] Glycal **10** was obtained by elimination of the 3′,5′-O-TBDMS-protected thymidine.[40] The Heck coupling is regio- and stereoselective to the corresponding β-anomer due to the sterically shielding TBDMS protecting group of glycal **10**, in combination with the ligands of the palladium catalyst. The catalyst Pd_2dba_3 in combination with the ligand Q-Phos achieved the highest yields of **11** (51%). Deprotection by $Et_3N{\cdot}HF$ gave **12**. Due to partial deprotection during the Heck coupling, **15** could only be purified after deprotection and a yield of 37% was obtained over two steps. As a byproduct, debromination of the thioxanthone was observed, which made purification more difficult due to π–π stacking interactions. The resulting 3′-keto derivatives **12** and **16** were reduced by $NaBH(OAc)_3$,[41] which is a stereoselective reduction, since the boron atom binds to the 5′-OH group by substituting an OAc group and thus the hydride can only attack the carbonyl carbon on one side, leading to the desired 2′-deoxyribofuranoside configuration. The C-nucleosides **1** and **2** were obtained in yields between 39% and 83%. For the subsequent solid-phase oligonucleotide synthesis, the C-nucleosides **1** and **2** were converted into the corresponding phosphoramidites **14** and **18** as DNA building blocks. First, the 5′-OH group was protected with DMT-Cl which gave **13** and **17** in yields between 33% and 71%. Although the DMT-Cl protecting group is known to selectively protect primary alcohols, protection of the 3′-OH group was also observed depending on the coupled chromophore, presumably due to different solubilities. Finally, the 5′-DMT protected nucleosides **13** and **17** were converted *via* phosphitylation into the respective phosphoramidites **14** and **18** in yields between 41% and 70%, respectively.

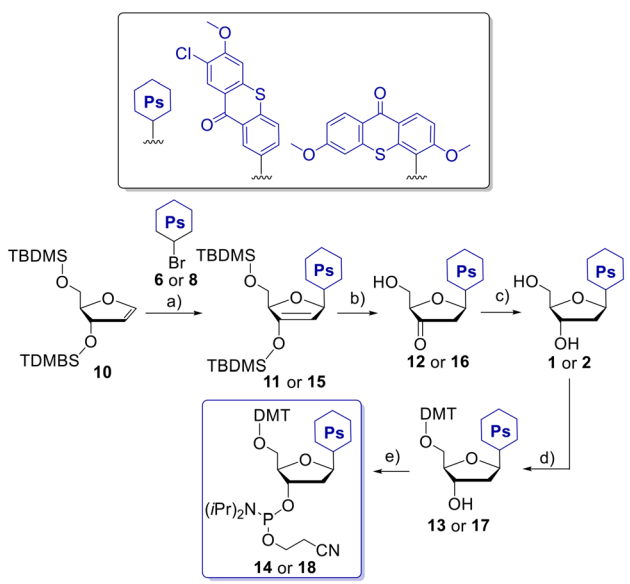

Scheme 2 Synthesis of C-nucleosides **1** and **2**, and their phosphoramidites **14** and **18** as DNA building blocks: (a) Pd_2dba_3 Q-Phos, Et_3N, DMF, 75 °C, and 72 h. (b) $Et_3N{\cdot}HF$, THF, rt, and 12 h. (c) $NaBH(OAc)_3$, MeCN : AcOH 1 : 1, 0 °C, and 1 h. (d) DMT-Cl, pyridine, rt, and 12 h. (e) 2-Cyanoethyl *N*,*N*-diisopropylchlorophosphoramidite, DIPEA, rt, and 4 h.

The photoactive and ternary DNA architectures **DNAX-*n*** (**X** = **1** or **2**, *n* = 0–3, Fig. 2) consisting of the template strand (TS) were prepared by phosphoramidite synthesis, into which the respective photosensitizers were placed, and two pieces of DNA counterstrands, each with a terminal T, were placed at the 3′ end of the strand marked with the ATTO dye (AS) and at the 5′ end of the counterstrand (GS). These neighboring Ts are therefore not covalently linked to each other, and the phosphodiester bond is absent. After selective excitation of the photosensitizer **X**, CPD damage can occur at this site, resulting in a covalent linkage of the opposing strands AS and GS through the cyclobutane between the Ts.[24] The sequence of **DNAX-*n*** was designed such that there is only exactly one designated CPD site. The DNA strand elongated by the CPD can be detected by RP-HPLC using the emission of ATTO550 dye at the 5′-end of the counterstrand AS in the fluorescence channel. This dye is photochemically sufficiently stable. The melting temperatures T_m of the hybridized DNA architectures **DNAX-*n*** were measured, which gave two values, T_{m1} of 11–15 °C (between TS and GS) and T_{m2} of 43–49 °C (between TS and AS) (Fig. S36 and Table S5†). This indicates complete hybridization of the DNA architectures below 10 °C. Due to the

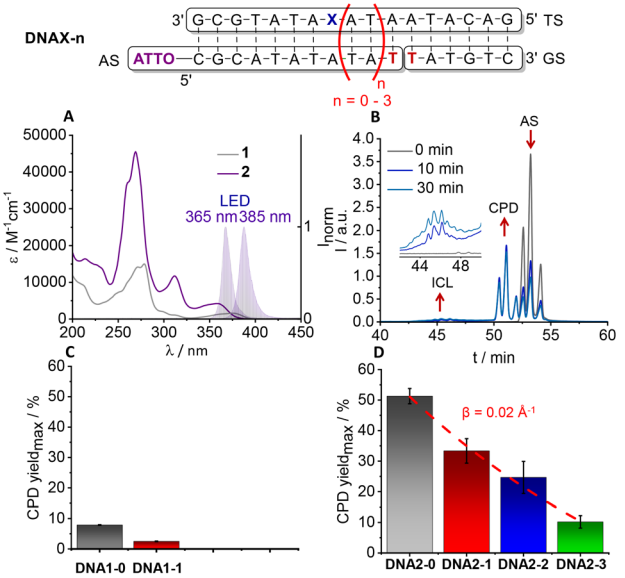

Fig. 2 Top: ternary DNA architectures **DNAX-*n***, consisting of the template strand (**TS**) containing the photosensitizer at position **X**, the complementary strand (**GS**), and the ATTO-labeled strand (**AS**). (A) UV/Vis absorption of thioxanthone nucleosides **1** (30 μM in MeCN) and **2** (12.5 μM in MeCN) with the normalized emission spectrum of the used 365 nm and 385 nm LEDs. (B) Exemplary chromatogram of the emission channel from the RP-HPLC of **DNA2-0** after 0 min, 10 min and 30 min of irradiation. (C and D) Maximum CPD yields for the respective distances of the DNA architectures **DNA1-*n*** and **DNA2-*n***. The CPD yields obtained in **DNA2-*n*** exhibit exponential distance dependence with a β-value of 0.02 Å^{-1}.

low melting temperature T_{m1} of the counterstrand GS, a small portion might be dissociated from the ternary DNA architecture. However, we assume that this experimental error can be neglected because it equally appears in all irradiation experiments. Circular dichroism was recorded at 10 °C representatively for the DNA architecture containing unmodified thioxanthone as the DNA reference where thymine replaces the photosensitizer **X** (**DNA0-0**). The circular dichroism result confirms the B-DNA conformation of the ternary DNA architectures (Fig. S37†).[42] The DNA architectures were exposed to 10 °C to ensure complete hybridization and placed in the absence of oxygen to avoid oxidative DNA damage. Due to the different UV/Vis absorption of the 2′-deoxynucleosides **1** and **2** (Fig. 2), **DNA1-*n*** was irradiated with a 385 nm LED, whereas **DNA2-*n*** was irradiated with a 365 nm LED. All irradiation experiments were performed in triplicate. During irradiation, aliquot samples were taken at defined time intervals and analyzed by RP-HPLC. The chemical CPD yields linking AS and GS as well as the chemical yields of interstrand crosslinks (ICLs) between TS and AS as a second product were quantified (see Fig. S46† and the corresponding calculations). All products were identified by LC-ESI-MS (Fig. S54–S79†). Despite the high photostability of the ATTO550 dye, some photobleaching of the dye was observed over time. However, it is assumed that the dye is bleached equally before as well as after CPD formation to the same extent, so this has no influence on the relative yields. As a negative control, the DNA architecture **DNA0-0** with a T instead of the photosensitizer **X** was used, for which no CPD damage was observed (Fig. S45 and 46†).

The C-nucleoside **1** has a local UV/Vis absorption maximum at 375 nm and is expected to have an increased triplet energy of E_T = 277 kJ mol^{-1}, estimated based on the hypsochromic shift compared to the unmodified thioxanthone C-nucleoside (Fig. 1).[20] We measured the phosphorescence of **DNA1-0** at 77 K and determined the triplet energy of **1** in DNA, E_T = 273 kJ mol^{-1}, which is slightly lower than expected (Fig. S81†). For **DNA1-0** and **DNA1-1**, the CPD yield showed a rapid increase over the first 2 h of irradiation, and then a plateau is reached. The plateau is most likely an equilibrium between CPD damage and CPD opening, as previously discussed.[24,43] The maximum CPD yields are reached after 6 h with 8% for **DNA1-0** and 2.5% for **DNA1-1**. Based on these low values, the architectures **DNA1-2** and **DNA1-3** were not prepared. As side products, ICLs were obtained in yields of 9% for **DNA1-0** (Fig. S47†) and 12% for **DNA1-1** after 6 h of irradiation (Fig. S48†). It is known from photoaffinity labeling that benzophenones and the structurally related xanthones are able to abstract an H atom through their triplet photochemistry, even from C–H bonds that are close.[44] In double-stranded DNA, this could be any C–H bond of the 2′-deoxyribofuranoside. The UV/Vis absorption of C-nucleoside **2** shows a local absorption maximum at 357 nm (Fig. 2). The hypsochromic shift compared to the previous thioxanthone as part of C-nucleoside **1** indicates an increase in triplet energy to E_T = 298 kJ mol^{-1} for photosensitizer **2**, as reported in the literature for thioxanthone **8**.[20] We measured the phosphorescence of **DNA2-0** at 77 K and determined the triplet energy of **2** in DNA, E_T = 288 kJ mol^{-1}, which is lower than expected (Fig. S80†). The CPD yields were again determined as a percentage over time. Due to the higher triplet energy E_T of **2** than that of **1**, **DNA2-0** (Fig. S49†) and **DNA2-1** (Fig. S50†) reach the CPD yield maximum of 51% and 33%, respectively, after only 20 min of irradiation. After reaching the maximum CPD yield, a significant decrease in CPD yield can be observed for **DNA2-0**. This effect can be explained by the possibility that CPDs can be reopened by a photoinduced electron transfer,[45–47] considering the reduction potential (E_{red} = 1.20 V *vs.* SCE)[48] as well as the oxidation potential (E_{ox} = 1.82 V)[48] of the photosensitizer **2** with respect to the corresponding potentials of the CPD (E_{ox} = 1.4–1.8 V, E_{red} = −1.93 V).[49] Using the simplified equation for the Gibbs energy of photoinduced electron transfer, $\Delta G = E_{ox} - E_{red} - E_{00}$ (without the Coulomb energy based on the polar environment of DNA) and with an E_{00} of 3.1 eV for **2**, only the oxidative opening of the CPDs by a hole transfer from the photoexcited **2*** is exergonic. Accordingly, an equilibrium between the formation and opening of CPDs is assumed that changes over the irradiation time. Since both CPD formation and cleavage are distance dependent, the equilibrium is reached later for **DNA2-2** (Fig. S51†) and **DNA2-3** (Fig. S52†), and the final CPD damage after 6 h of irradiation is lower, compared to **DNA2-0** and **DNA2-1**. When the maximum CPD

yield is plotted against the distances of the DNA architectures **DNA2-*n*** after 20 min of irradiation, a weak exponential distance dependence can be observed, with a β value of 0.02 Å^{-1} (Fig. 2). This value is low, especially in the context of a Dexter-type energy transfer.

Discussion

Both photosensitizers, **1** and **2**, were incorporated into similar DNA architectures and into the same sequential environment so that the influence of structural properties of the DNA on the distance dependence of CPD formation can be ruled out. Thus, the different distance dependencies of the energy transfer must be explained by different photophysical properties, mainly the triplet energies E_T. Xanthone has a high triplet energy of E_T = 310 kJ mol^{-1} (ref. 21) and is able to induce CPD formation over a distance of up to 7 base pairs.[24] The distance dependence for the energy migration over the 7 base pairs is extremely low with β = 0.05 Å^{-1}.[24] The methoxy-substituted thioxanthone as a photosensitizer in C-nucleoside **2** has a lower triplet energy of E_T = 288 kJ mol^{-1}. This seems to have no major effect as the distance dependence of the energy transfer in the DNA architectures **DNA2-*n*** occurs with an – within the experimental error – equally low β-value of 0.02 Å^{-1}. We therefore propose that the energy migration in **DNA2-*n*** occurs as energy hopping over the A–T pairs, similar to the xanthone–DNA architectures.[24] In principle, both intrastrand energy hopping and interstrand energy hopping can occur and form CPDs. It was calculated that intrastrand energy transport from T to T over an intervening A, mediated by super-exchange coupling, is favored compared to interstrand energy transport between consecutive Ts.[50] It was suggested that exchanging an A–T pair for a C–G pair could provide further insight into the triplet energy mechanism,[50] and we hypothesized that intrastrand energy transport may also occur *via* other bases. For such an experiment, a modified DNA architecture **DNA2-2-G/C** was used, in which one A–T pair was replaced with a C–G pair (Fig. S53†). In this case, only intrastrand triplet energy transport was possible, so that triplet energy from T to T had to take place *via* intermediate C. In fact, the amount of CPD damage observed in **DNA2-2-G/C** was in a similar range to that in **DNA2-2**, evidencing that the triplet transport mechanism proceeds *via* intrastrand energy hopping and can occur *via* both A and C. Finally, the triplet energy of the photosensitizer in C-nucleoside **1** can be estimated to be E_T = 273 kJ mol^{-1} due to the local absorption maximum of 375 nm. This value is only slightly above the triplet energy E_T = 267 kJ mol^{-1} of Ts in DNA. The DNA architecture **DNA1-0** shows a maximum CPD yield of only 8% because the energy difference ΔE_T is very small. Taken together, these results show clearly that only the triplet energy E_T of the photosensitizer incorporated into the DNA is decisive for whether CPDs can be induced and how much CPDs are formed. We know from methoxyxanthone as a photosensitizer in DNA that this type of triplet photochemistry is very inefficient, with reaction quantum yields below 0.1%.[51]

The rate of energy transfer might depend exponentially on the triplet energy E_T, whereas the extinction and photon flux are more likely to be linear. Taken together, this might give the observed correlation of the CPD yield. The higher the triplet energy E_T of the photosensitizer and the greater the ΔE_T compared to T, the more the balance shifts in favor of the excited T*. The comparison with the CPD yields described in the literature for the triplet sensitizer triphenylene[24] shows a good agreement with the dependence of CPD formation described here (Fig. 3). The CPD yields observed with 4-methylbenzophenone[52] and 4-methoxybenzophenone[52] as photosensitizers in DNA are lower probably due to the poorer stacking of these chromophores and their twisted conformation. Taken together, the results also match the value determined for the triplet energy of thymine (E_T = 267 kJ mol^{-1}) as the threshold.[33] It indicates the lower limit above which CPD damage can be detected. Between E_T = 267 kJ mol^{-1} and 310 kJ mol^{-1}, there is

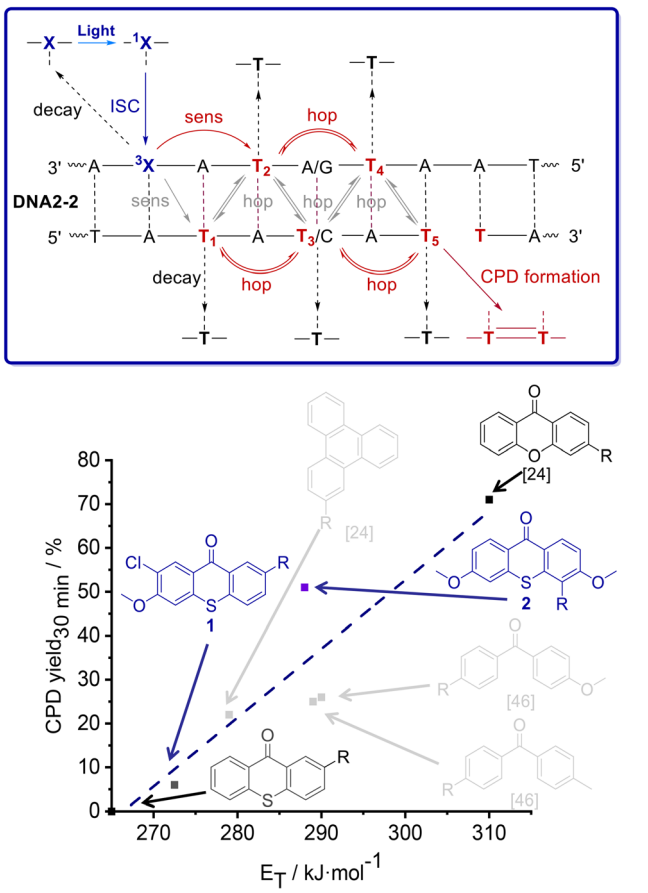

Fig. 3 Top: proposed energy transfer mechanism leading to remote CPD formation in DNA, most likely driven by preferential intrastrand triplet energy transfer (red) between thymine bases. Bottom: maximum CPD yields of different photosensitizers after 30 min of irradiation, plotted against their respective triplet energies E_T. A correlation between the maximum CPD yield and the triplet energy E_T of the photosensitizers can be observed, illustrated by the dashed line. The triplet energies of thioxanthones **1** and **2** were measured in DNA, whereas the triplet energies of terphenylene and benzophenones are values of the chromophores in organic solvent obtained from the literature.

a clear correlation between E_T and CPD yield. This correlation is simplified and does not take into consideration that extinction, quantum yields of intersystem crossing and triplet lifetimes of the photosensitizers are different. In addition, of course, it is not universal and applies only to identical DNA sequences in the photoactive DNA architectures, which we used for all different chromophores. Nevertheless, the observed correlation is striking and evidences that the triplet energy E_T is a key parameter for the triplet-dependent CPD formation in DNA.

Conclusions

Our results show that thioxanthones are tunable photosensitizers for studying the formation of triplet-induced CPD damage in DNA by energy transfer. To probe the gap between the triplet energy of xanthone, E_T = 310 kJ mol^{-1}, and of thioxanthone, E_T = 265 kJ mol^{-1}, which is nearly identical to the energy gap between T monophosphate and T in DNA, we synthesized the C-nucleosides **1** and **2** with two differently modified thioxanthones. For the subsequent solid-phase oligonucleotide synthesis, the C-nucleosides **1** and **2** were converted into the corresponding phosphoramidites **14** and **18** as DNA building blocks. Within the mentioned triplet energy range, the methoxy-substituted thioxanthone as a photosensitizer in C-nucleoside **2** has a high triplet energy of E_T = 288 kJ mol^{-1}. We observed high CPD yields and CPD formation over up to 6 A–T pairs in DNA architectures **DNA2-*n***. The distance dependence is characterized by a low β-value of 0.02 Å^{-1}. We therefore propose that the energy migration in **DNA2-*n*** occurs as energy hopping over the A–T pairs, similar to the xanthone–DNA architectures.[24] The triplet energy of the photosensitizer in C-nucleoside **1** is low, E_T = 273 kJ mol^{-1}, only slightly above the threshold for DNA photosensitization set by the triplet energy of T in DNA, E_T = 267 kJ mol^{-1}. Because the energy difference ΔE_T is very small, the DNA architecture **DNA1-0** shows only low amounts of CPDs. Taken together, these results show clearly that the triplet energy E_T of the photosensitizer incorporated into the DNA is not only decisive for whether CPDs can be induced (based on the threshold E_T = 270 kJ mol^{-1}) or not, but also how much CPDs are formed. The higher the triplet energy E_T of the photosensitizer and the greater the ΔE_T compared to T, the more CPDs are formed. Together with xanthone and thioxanthone, a nearly linear relationship between ΔE_T and maximum CPD yield is obtained in a simplified manner. This relationship is important for potential photosensitizers as part of antibiotics and sunscreens, or for natural DNA modifications with photosensitizers.

Author contributions

SH performed the experiments. JAM performed 77 K emission measurements. HAW and CK supervised the research and HAW wrote the manuscript.

Data availability

The data supporting this article have been included as part of the ESI.†

Conflicts of interest

There are no conflicts to declare.

Acknowledgements

Financial support by the KIT is gratefully acknowledged.

References

1 J.-S. Taylor, *Acc. Chem. Res.*, 1994, **27**, 76–82.
2 G. P. Pfeifer and A. Besaratinia, *Photochem. Photobiol. Sci.*, 2012, **11**, 90–97.
3 J. Cadet and T. Douki, *Photochem. Photobiol. Sci.*, 2018, **17**, 1816–1841.
4 K. Heil, D. Pearson and T. Carell, *Chem. Soc. Rev.*, 2011, **40**, 4271–4278.
5 E. Sage, P.-M. Girard and S. Francesconi, *Photochem. Photobiol. Sci.*, 2012, **11**, 74–80.
6 J. Cadet, A. Grand and T. Douki, *Top. Curr. Chem.*, 2015, **356**, 249–276.
7 T. Gustavsson and D. Markovitsi, *Acc. Chem. Res.*, 2021, **54**, 1226–1235.
8 N. K. Schwalb and F. Temps, *Science*, 2008, **322**, 243–245.
9 Y. Zhang, K. d. L. Harpe, A. A. Beckstead, R. Improta and B. Kohler, *J. Am. Chem. Soc.*, 2015, **137**, 7059–7062.
10 D. B. Bucher, B. M. Pilles, T. Carell and W. Zinth, *Proc. Natl. Acad. Sci. U. S. A.*, 2014, **111**, 4369–4374.
11 I. Buchvarov, Q. Wang, M. Raytchev, A. Trifonov and T. Fiebig, *Proc. Natl. Acad. Sci. U. S. A.*, 2007, **104**, 4794–4797.
12 C. T. Middleton, K. d. L. Harpe, C. Su, Y. K. Law, C. E. Crespo-Hernandez and B. Kohler, *Annu. Rev. Phys. Chem.*, 2009, **60**, 217–239.
13 W. J. Schreier, T. E. Schrader, F. O. Koller, P. Gilch, C. E. Crespo-Hernandez, V. N. Swaminathan, T. Carell, W. Zinth and B. Kohler, *Science*, 2007, **315**, 625–629.
14 S. Mouret, C. Baudouin, M. Charveron, A. Favier, J. Cadet and T. Douki, *Proc. Natl. Acad. Sci. U. S. A.*, 2006, **103**, 13765–13770.
15 J. Cadet, T. Douki, J.-L. Ravanat and P. D. Mascio, *Photochem. Photobiol. Sci.*, 2009, **8**, 903–911.
16 M. C. Cuquerella, V. Lhiaubet-Vallet, J. Cadet and M. A. Miranda, *Acc. Chem. Res.*, 2012, **45**, 1558–1570.
17 V. Lhiaubet-Vallet, M. C. Cuquerella, J. V. Castell, F. Bosca and M. A. Miranda, *J. Phys. Chem. B*, 2007, **111**, 7409–7414.
18 L. Allahkaram, A. Monari and E. Dumont, *Photochem. Photobiol.*, 2022, **98**, 633–639.
19 A. Blasco-Brusola, I. Vayá and M. A. Miranda, *J. Org. Chem.*, 2020, **85**, 14068–14076.

20 L. D. Elliott, S. Kayal, M. W. George and K. Booker-Milburn, *J. Am. Chem. Soc.*, 2020, **142**, 14947–14956.
21 W. G. Herkstroeter, A. A. Lamola and G. S. Hammond, *J. Am. Chem. Soc.*, 1964, **86**, 4537–4540.
22 N. F. Nikitas, P. L. Gkizis and C. G. Kokotos, *Org. Biomol. Chem.*, 2021, **19**, 5237–5253.
23 D. Armesto, M. J. Ortiz, A. R. Agarrabeitia and N. El-Boulifi, *Angew. Chem.*, 2005, **117**, 7917–7919.
24 S. Häcker, M. Schrödter, A. Kuhlmann and H.-A. Wagenknecht, *JACS Au*, 2023, **3**, 1843–1850.
25 L. A. Ortiz-Rodriguez and C. E. Crespo-Hernández, *Chem. Sci.*, 2020, **11**, 11113–11123.
26 Y. Xiao, X. Huang, J. Feng, Z. Ni, L. Gai, X. Xiao, X. Sui and H. Lu, *Dyes Pigm.*, 2022, **200**, 110167.
27 A. Tiwari, I. Mondal and U. Pal, *RSC Adv.*, 2015, **5**, 31415–31421.
28 N. Pearce, E. S. Davies, R. Horvath, C. R. Pfeiffer, X.-Z. Sun, W. Lewis, J. McMaster, M. W. George and N. R. Champness, *Phys. Chem. Chem. Phys.*, 2018, **20**, 752–764.
29 J. D. Williams, M. Nakano, R. Gérardy, J. A. Rincón, O. De Frutos, C. Mateos, J.-C. M. Monbaliu and C. O. Kappe, *Org. Process Res. Dev.*, 2018, **23**, 78–87.
30 R. Alonso and T. Bach, *Angew. Chem.*, 2014, **126**, 4457–4460.
31 F. Pecho, Y. Q. Zou, J. Gramüller, T. Mori, S. M. Huber, A. Bauer, R. M. Gschwind and T. Bach, *Chem. – Eur. J.*, 2020, **26**, 5190–5194.
32 R. Kleinmans, T. Pinkert, S. Dutta, T. O. Paulisch, H. Keum, C. G. Daniliuc and F. Glorius, *Nature*, 2022, **605**, 477–482.
33 F. Bosca, V. Lhiaubet-Vallet, M. C. Cuquerella, J. V. Castell and M. A. Miranda, *J. Am. Chem. Soc.*, 2006, **128**, 6318–6319.
34 S. Häcker, T. J. B. Zähringer, H.-A. Wagenknecht and C. Kerzig, *JACS Au*, 2025, DOI: **10.1021/jacsau.5c00364**.
35 W. D. Watson, *J. Org. Chem.*, 1985, **50**, 2145–2148.
36 M. Kharasch and H. C. Brown, *J. Am. Chem. Soc.*, 1939, **61**, 2142–2150.
37 S. Kajigaeshi and T. Kakinami, *Ind. Chem. Libr.*, 1995, **7**, 29–48.
38 M. Hocek, *Chem. Rev.*, 2009, **109**, 6729–6764.
39 J. G. Doyle Daves, *Acc. Chem. Res.*, 1990, **23**, 201–206.
40 M. A. Cameron, S. B. Cush and R. P. Hammer, *J. Org. Chem.*, 1997, **62**, 9065–9069.
41 N. Joubert, R. Pohl, B. Klepetárová and M. Hocek, *J. Org. Chem.*, 2007, **72**, 6797–6805.
42 M. Vorlíčková, I. Kejnovská, K. Bednářová, D. Renčiuk and J. Kypr, *Chirality*, 2012, **24**, 691–698.
43 M. Schrödter and H.-A. Wagenknecht, *J. Am. Chem. Soc.*, 2024, **146**, 20742–20749.
44 F. Kotzyba-Hibert, I. Kapfer and M. Goeldner, *Angew. Chem., Int. Ed. Engl.*, 1995, **34**, 1296–1312.
45 C. Helene and M. Charlier, *Biochimie*, 1971, **53**, 1175–1180.
46 D. B. Bucher, C. L. Kufner, A. Schlueter, T. Carell and W. Zinth, *J. Am. Chem. Soc.*, 2016, **138**, 186–190.
47 M. R. Holman, T. Ito and S. E. Rokita, *J. Am. Chem. Soc.*, 2006, **129**, 6–7.
48 K. Zhu, T. Ohtani, C. B. Tripathi, D. Uraguchi and T. Ooi, *Chem. Lett.*, 2019, **48**, 715–717.
49 C. A. M. Seidel, A. Schulz and M. H. M. Sauer, *J. Phys. Chem.*, 1996, **100**, 5541–5553.
50 L. Blancafort and A. A. Voityuk, *Phys. Chem. Chem. Phys.*, 2018, **20**, 4997–5000.
51 A. Kuhlmann, L. Bihr and H.-A. Wagenknecht, *Angew. Chem., Int. Ed.*, 2020, **59**, 17378–17382.
52 L. Antusch, N. Gaß and H.-A. Wagenknecht, *Angew. Chem., Int. Ed.*, 2017, **56**, 1385–1389.